A Journal of the Gesellschaft Deutscher Chemiker
Angewandte Chemie
GDCh
International Edition
www.angewandte.org

Accepted Article

Title: Indirect CO2 methanation: hydrogenolysis of cyclic carbonates catalyzed by Ru-modified zeolite produces methane and diols

Authors: Wei-Tse Lee, Antoine Philippe van Muyden, Felix Daniel Bobbink, Zhangjun Huang, and Paul J. Dyson

To be cited as: *Angew. Chem. Int. Ed.* 10.1002/anie.201811086
Angew. Chem. 10.1002/ange.201811086

Link to VoR: http://dx.doi.org/10.1002/anie.201811086
http://dx.doi.org/10.1002/ange.201811086

WILEY-VCH

10.1002/anie.201811086

Indirect CO_2 methanation: hydrogenolysis of cyclic carbonates catalyzed by Ru-modified zeolite produces methane and diols

Wei-Tse Lee+, Antoine P. van Muyden+, Felix D. Bobbink, Zhangjun Huang, Paul J. Dyson*

Abstract: We report a ruthenium-modified zeolite which efficiently transforms propylene carbonate to propylene glycol and methane, under solvent-free conditions. The catalyst achieves high product selectivity and no significant ageing effect was observed after multiple cycles. The resulting liquid product (water-containing glycol) can be directly used as anti-freeze solution and the gas phase can directly be used as an energy carrier in the form of H_2-enriched methane. This process efficiently bridges energy storage and an important chemical synthesis under sustainable (CO_2 consuming) conditions.

The utilization of carbon dioxide (CO_2) as a non-toxic and abundant (35 GT/year from human emissions) C_1 feedstock has attracted significant attention in the transition towards a more sustainable chemical industry.[1,2] Value-added products, and in particular energy-related chemicals derived from CO_2, are coveted owing to the escalating demand of global fuel supply.[3,4] However, the high stability of CO_2 hinders its efficient utilization.[5–7]

Methanation is a typical example of direct CO_2 transformation (Figure 1**a**) with the process requiring high temperatures (250-300 °C) and high pressures (50-100 atm) and a catalyst.[8,9] Catalysts that directly reduce CO_2 into methanol[10–12] or formic acid[13,14] under relatively mild conditions have also been developed.

Indirect methanation methods employing "relay molecules" convert CO_2 to CH_4 via distinct steps (Figure 1**b**, typically below 200 °C). Organic carbonates are suitable relay molecules due to their low-toxicity and facile synthesis from CO_2 via the cycloaddition of CO_2 into epoxides.[15–18] In the second step the corresponding diol and methane are produced, with the diol being a value-added product compared to the epoxide starting material.[19,20] Industrially, the production of ethylene glycol is achieved via the OMEGA process via the reaction of CO_2 with ethylene oxide, followed by hydrolysis of the carbonate to generate the glycol and regenerate CO_2.[21] Additional value can be obtained by coupling the OMEGA process with a reduction step, thus simultaneously valorizing CO_2.

In a pioneering study, Milstein reported the hydrogenolysis of dimethyl carbonate (DMC) into methanol employing a homogeneous Ru(II)-pincer catalyst (see Table S1 for the reaction conditions).[22] Heterogeneous catalysts able to convert cyclic organic carbonates with high selectivity have also been reported by other groups (Table S1).[23–25] Very recently, three examples of homogeneous catalysts based on a non-noble metal center (manganese) have been reported that transform organic carbonates into diols and methanol in high yields (see Table S2).[26–28]

A limitation of the aforementioned approaches is that the methanol and glycol-products must be separated prior to further utilization, which is an energy intensive step. Hence, we decided to develop a catalytic process that converts cyclic carbonates directly into methane and diols, producing value-added gaseous- and liquid-phases that do not require further separation. To achieve this goal, we relied on a well-established type of heterogeneous catalyst (Ru nanoclusters stabilized by zeolites). These types of catalysts were previously found to display excellent properties and long-term stability, for example in the hydrogenation of aromatics and CO_2 or in NO_x absorption.[29–33] The catalyst is robust and operates under solvent-free reaction conditions to afford hydrogen-enriched natural gas (HENG)[34,35] and propylene glycol (PG) water mixture, a ready-to-use anti-freeze solution.

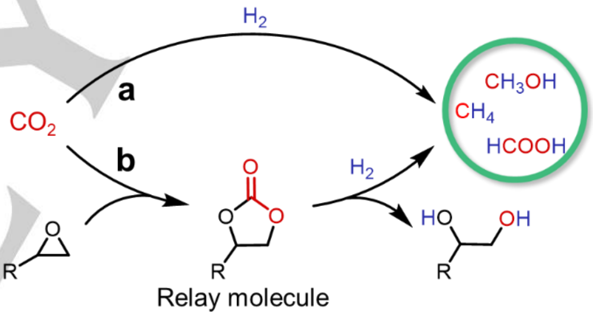

Figure 1. a) Direct and **b)** Indirect CO_2 utilization pathways.

Results and discussions

Based on previous studies, we evaluated both Cu and Ru nanoparticles (NPs) immobilized on a faujasite type x zeolite framework (FAU-zeolite). Despite Cu being one of the most prominent metals for CO_2-related reactions, the Cu catalyst showed very limited reactivity under the experimental reaction conditions (see Table S4, SI), presumably due to the large size of the particles.[23–25,36] In contrast, the Ru catalyst showed promising activity and was investigated further.

We employed a cation exchange procedure (Figure 2) followed by reduction with excess $NaBH_{4(aq)}$.[31] This way, the reduced metal ions aggregate on the Ru atoms present into the zeolite framework resulting in embedded NPs (to produce the solid phase catalyst termed Ru-FAU, Figure 2**c**).[31,37]

---

[a] W.-T. Lee, A. P. van Muyden, Dr. F. D. Bobbink, Dr. Z. Huang, Prof. Dr. P. J. Dyson Institut des Sciences et Ingénieuries Chimique, École Polytechnique Fédérale de Lausanne (EPFL), 1015 Lausanne, Switzerland. Email: pjd@epfl.ch
+: equal contribution

Supporting information for this article is given via a link at the end of the document.

10.1002/anie.201811086

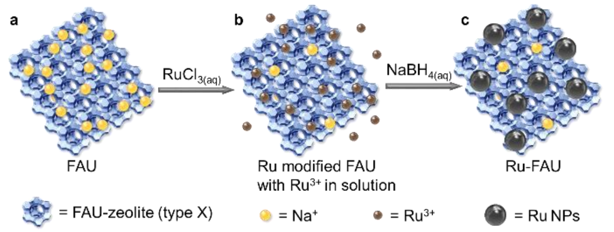

Figure 2. Illustration of the synthesis of solid phase Ru catalyst **a)** FAU-zeolite (type X); **b)** Ion exchange of Na$^+$ by Ru^{3+}; **c)** Ru-FAU.

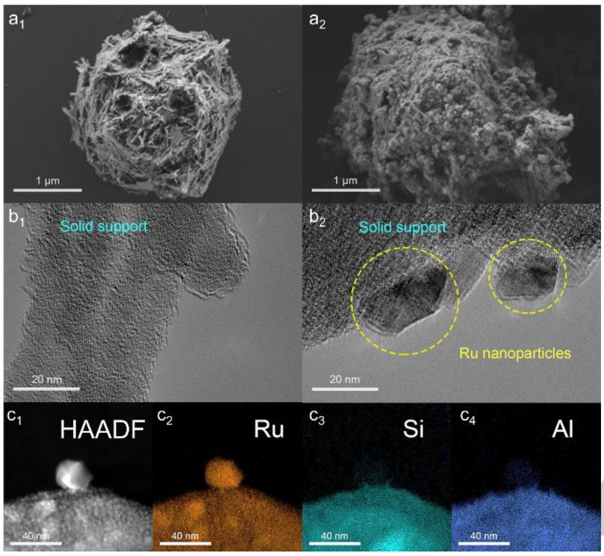

Figure 3. a$_1$) SEM image of the FAU-zeolite support; **a$_2$)** SEM image of the Ru-FAU catalyst; **b$_1$)** HRTEM image of the FAU-zeolite support; **b$_2$)** HRTEM image of the Ru-FAU catalyst, yellow circle: crystalline Ru nano-structures; **c$_1$)** HAADF image of the Ru-FAU catalyst; **c$_2$, c$_3$, c$_4$)** STEM elemental mapping of the Ru-FAU catalyst: Ru, Si, Al, respectively.

The FAU-zeolite (in the absence of Ru NPs) has a particle diameter ranging from 1.5 to 3.0 µm (Figure S1, SI), which remains essentially the same in the Ru-FAU catalyst (cf. Figure 3**a$_1$** vs. **a$_2$**). HRTEM images reveal that crystalline Ru NPs protrude from the FAU-zeolite surface with diameters typically ranging from 10 to 20 nm (see Figure 3**b$_1$** and 3**b$_2$** for a comparison between the FAU-zeolite and the Ru-FAU catalyst, and Figures S2-S3 for further details).

The protruding Ru NPs were further analyzed by high-angle annular dark-field scanning transmission electron microscopy (HADDF-STEM, Figure 3) together with STEM-energy-dispersive X-ray spectrometry (STEM-EDX, Figures S5-S7). Strong Ru signals were associated with these structures (Figure 3**c$_1$** and **c$_2$**), whereas Si and Al are absent within the protruding Ru nanostructure (Figure 3**c$_3$** and **c$_4$**). Mapping indicates that the pores of the FAU-zeolite are partially filled with Ru (Figure 3**c$_2$**), firmly embedding the Ru NPs on the support.

Brunauer–Emmett–Teller (BET) analysis showed that the porosity of the FAU-zeolite decreases upon formation of the Ru NPs. The FAU-zeolite displays a surface area of 423.32 m^2/g (Figure S9**a**) and the Ru-FAU catalyst has a similar adsorption curve, i.e. the adsorption of a microporous material, but with decreased N_2 adsorption and a surface area of 214.45 m^2/g. This decrease in adsorption indirectly confirms that Ru NPs partially fill the FAU-zeolite pores and has been observed in similar types of supported metal catalysts.[38]

Powder X-ray diffraction (powder-XRD) further demonstrates the crystalline nature of the Ru-FAU catalyst (Figure S9**b**) and showed that the native structure of the FAU support is conserved.[31] Broadening of the peaks combined with a decrease in peak intensity suggests that the different crystalline frameworks are entangled and slightly amorphous.[39,40]

X-ray photoelectron spectroscopy (XPS) revealed the presence of Ru species at 4.4%±0.1% on the surface of the Ru-FAU catalyst. (Ru(3p) was selected to represent the elemental concentration, see SI for details). As expected, aluminum silicate is the major component of both solids (Table S2). Note the signal of Na (1s, 1071.50 eV) was chosen as the calibration due to the lack of suitable C(1s) species.[41] Mg^{2+} ions are also present in the support material (Figure S8). The native cations (Na$^+$ and Mg^{2+}) are observed by XPS before and after ion exchange indicating that the exchange process is not quantitative under the conditions used herein (Table S2). The cation loading was further examined by means of ICP-OES analysis with 7.3 wt% of Ru, 8.2 wt% of Na and 0.9 wt% of Mg determined.

The Ru-FAU catalyst was initially studied using propylene carbonate (PC) as the substrate with the optimization results compiled in Table S3. Propylene glycol (PG) and water are the major liquid products with traces of 2-propanol (^{i}PrOH) and ethanol (EtOH) detected. At 150 and 160 °C conversion is low (13% and 40% respectively, see Figure 4, left), whereas at higher temperatures (≥ 170 °C) conversions were near-quantitative (97 - 99%, see Figures S12-S13 for representative ^{1}H NMR spectrum). At 180 °C, however, the PG product is converted into gaseous products lowering the yield (Table S3, entry **4**). Consequently, 170 °C (Table S3 entry **3**) was selected as the optimum reaction temperature for subsequent studies. This temperature is similar to that used in other reports describing the hydrogenation of cyclic carbonate.[36]

The main gaseous product is methane with traces of propane (2%) and CO_2 (1%) detected (Figure 4, right, and Figure S10). CO_2 results from the hydrolysis of the carbonate by the water produced during the reaction. To exclude that adsorbed water into the zeolite framework leads to the hydrolysis of PC the reaction was performed under a N_2 atmosphere and CO_2 and PG were not detected. Presumably, the acidic site present in the Ru-FAU catalyst is also able to promote reductive dehydration, rationalizing the formation of propane and the absence of MeOH, in sharp contrast with previous reports that produce MeOH selectively.[26,36]

The influence of hydrogen pressure was studied with the conversion of PC ranging from 84% at 40 bar to 98% at 80 bar. Hydrogen pressure strongly impacts on the selectivity of gaseous products, with less CO_2 formed at higher hydrogen pressures (Table S3, entries **5-8**). This indicates that either hydrolysis is suppressed or CO_2 is reduced via a Sabatier-type pathway under

10.1002/anie.201811086

the reaction conditions.[34] In this respect, a reaction using CO_2 as substrate demonstrated that Ru-FAU is also able to catalyze the methanation of CO_2 at temperatures well below those typically used in the Sabatier process (Table 1, entry **4**).[42,43] Remarkably, higher hydrogen pressure also favored the conversion of PG to gaseous products resulting in a lower yield of PG (Table S3, entry **8**). Consequently, 70 bar of H_2 was chosen as the optimal applied pressure.

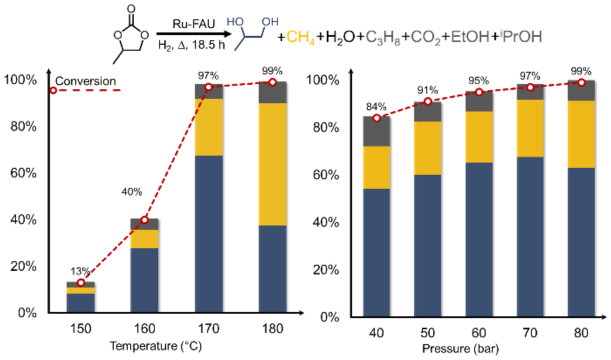

Figure 4. Hydrogenolysis of propylene carbonate (PC) to propylene glycol (PG) and methane. Reaction conditions: PC (1021 mg, 10.0 mmol), Ru-FAU (100 mg; Ru loading = 0.072 mmol), H_2 (70 bar), 18.5 h. Right: reaction temperature: 170 °C. * Conversions and yields were determined by ^1H NMR spectroscopy with dibromomethane as an internal standard in d^6-acetone.

The substrate scope was extended to ethylene carbonate (EC) and a non-cyclic carbonate, i.e dimethyl carbonate (DMC), which are converted in 99% and 91%, respectively, under the optimized reaction conditions (Table 1, entries **1-2**). When using DMC, only traces of MeOH were present implying that MeOH is also transformed into methane (confirmed in Table 1, entry **3**). As expected, methane and ethylene glycol (EG) were concomitantly generated in the case of EC.

Table 1. Conversion of different substrates by the Ru-FAU catalyst.

Entry	Substrate	Conv. [%]	Liquid prod. [%]	Gas prod. [%] CH_4 – CO_2
1	DMC	91	MeOH, 2	68 – 0
2	EC	99	EG, 62 EtOH, 1	30 – 1
3	MeOH	96	None	87 – 0
4[a]	CO_2	56	None	56 – 44

Reaction conditions: Substrate (10 mmol), Ru-FAU(100 mg; Ru loading = 0.072 mmol), H_2 (70 bar), 170 °C, 18.5 h. [a] CO_2 (20 bar), H_2 (70 bar), 200 ºC; Conversions and yields were determined by ^1H NMR spectroscopy with dibromomethane used as an internal standard in d^6-acetone or d^6-DMSO.

To evaluate the robustness of the catalyst, recycling experiments were performed with a total of 5 catalytic cycles of the Ru-FAU catalyst demonstrating that the combined PG and methane yields remain almost constant (Table S5, Figure S11).[44] However, the PG yield decreases as it is converted to methane, indicating that the catalyst becomes more active over time. The first three reaction cycles could be considered as activation steps after which the product yields remain constant.

As a comparison, a commercial Ru/C was tested, which led to 69% conversion of PC and produced PG and methane (Table S4, entry **4**), but upon recycling the activity decreased markedly and PG was obtained in a lower yield (Table S4, entry **5**). The FAU-zeolite or $RuCl_3$ alone are able to convert PC, but are not selective towards glycol and methane (Table S4 entries **7-8**) No conversion was achieved by these three catalysts under nitrogen, confirming that the potential presence of water in the catalyst does not participate in the hydrolysis of the cyclic carbonate.

In summary, Ru modified FAU-zeolites efficiently catalyze the indirect methanation of CO_2 via the hydrogenolysis of PC. The reaction results in the production of valuable gaseous energy carrier, i.e. hydrogen enriched methane, together with a liquid phase composed of PG and water that can be directly used as antifreeze solution following further dilution with water. The catalyst is easily recovered and recycled. This process represents a feasible extension to OMEGA process, bridging chemical production with efficient energy storage and, at the same time, valorizing CO_2 and with the added advantage of no separation of the products required.

Experimental Section

Experimental details are provided in the Supporting Information.

Acknowledgements

We thank the EPFL, Swiss National Science Foundation and the Swiss Competence Center for Energy Research (SCCER) on Heat and Electricity Storage for financial support. Daniel Sun, Alexander Stephens, José Bila, Pierre Mettraux, and Pascal Schouwink are thanked for help with the BET, XPS and XRD analysis.

Keywords: Sustainable chemistry, heterogeneous catalysis, ruthenium nanoparticles, hydrogenolysis, carbon dioxide, organic carbonates.

References

[1] A. Tlili, X. Frogneux, E. Blondiaux, T. Cantat, *Angew. Chemie - Int. Ed.* **2014**, *53*, 2543–2545.

[2] T. C. Merkel, H. Lin, X. Wei, R. Baker, *J. Memb. Sci.* **2010**, *359*, 126–139.

[3] A. Goeppert, M. Czaun, J. P. Jones, G. K. Surya Prakash, G. A. Olah, *Chem. Soc. Rev.* **2014**, *43*, 7995–8048.

[4] G. A. Olah, *Angew. Chemie Int. Ed.* **2005**, *44*, 2636–2639.

[5] Z. Li, J. Wang, Y. Qu, H. Liu, C. Tang, S. Miao, Z. Feng, H. An, C. Li, *ACS Catal.* **2017**, *7*, 8544–8548.

[6] Y. Jiao, Y. Zheng, P. Chen, M. Jaroniec, S. Z. Qiao, *J. Am. Chem. Soc.* **2017**, *139*, 18093–18100.

[7] P. Gao, S. Li, X. Bu, S. Dang, Z. Liu, H. Wang, L. Zhong, M. Qiu, C. Yang, J. Cai, et al., *Nat. Chem.* **2017**, *9*, 1019–1024.

[8] J. C. J. Bart, R. P. A. Sneeden, *Catal. Today* **1987**, *2*, 1–124.

[9] J. Chen, L. Falivene, L. Caporaso, L. Cavallo, E. Y. X. Chen, *J. Am. Chem. Soc.* **2016**, *138*, 5321–5333.

[10] C.-S. Li, G. Melaet, W. T. Ralston, K. An, C. Brooks, Y. Ye, Y.-S.

Liu, J. Zhu, J. Guo, S. Alayoglu, et al., *Nat. Commun.* **2015**, *6*, 6538.

[11] F. Studt, I. Sharafutdinov, F. Abild-Pedersen, C. F. Elkjær, J. S. Hummelshøj, S. Dahl, I. Chorkendorff, J. K. Nørskov, *Nat. Chem.* **2014**, *6*, 320–324.

[12] J. Graciani, K. Mudiyanselage, F. Xu, A. E. Baber, J. Evans, S. D. Senanayake, D. J. Stacchiola, P. Liu, J. Hrbek, J. F. Sanz, et al., *Science,.* **2014**, *345*, 546–550.

[13] S. Gao, Y. Lin, X. Jiao, Y. Sun, Q. Luo, W. Zhang, D. Li, J. Yang, Y. Xie, *Nature* **2016**, *529*, 68–71.

[14] S. Moret, P. J. Dyson, G. Laurenczy, *Nat. Commun.* **2014**, *5*, 4017.

[15] S. S. Zhang, *J. Power Sources* **2006**, *162*, 1379–1394.

[16] F. D. Bobbink, P. J. Dyson, *J. Catal.* **2016**, *343*, 52–61.

[17] T. Sakakura, J. C. Choi, H. Yasuda, *Chem. Rev.* **2007**, *107*, 2365–2387.

[18] T. Sakakura, K. Kohno, *Chem. Commun.* **2009**, 1312–1330.

[19] K. Knop, R. Hoogenboom, D. Fischer, U. S. Schubert, *Angew. Chemie - Int. Ed.* **2010**, *49*, 6288–6308.

[20] J. Zhu, *Biomaterials* **2010**, *31*, 4639–4656.

[21] G. J. (Jimmy); Milligen, Han van ;VanderWilp, Brian; Wells, *Shell Glob. Solut.* **2016**, 1–12.

[22] E. Balaraman, C. Gunanathan, J. Zhang, L. J. W. Shimon, D. Milstein, *Nat. Chem.* **2011**, *3*, 609–614.

[23] C. Lian, F. Ren, Y. Liu, G. Zhao, Y. Ji, H. Rong, W. Jia, L. Ma, H. Lu, D. Wang, et al., *Chem. Commun.* **2015**, *51*, 1252–1254.

[24] X. Chen, Y. Cui, C. Wen, B. Wang, W. L. Dai, *Chem. Commun.* **2015**, *51*, 13776–13778.

[25] H. Liu, Z. Huang, Z. Han, K. Ding, H. Liu, C. Xia, J. Chen, *Green Chem.* **2015**, *17*, 4281–4290.

[26] V. Zubar, Y. Lebedev, L. M. Azofra, L. Cavallo, O. El-Sepelgy, M. Rueping, *Angew. Chemie Int. Ed.* **2018**,doi :10.1002/anie.201805630.

[27] A. Kaithal, M. Hölscher, W. Leitner, *Angew. Chemie Int. Ed.* **2018**, doi: 10.1002/anie.201808676.

[28] A. Kumar, T. Janes, N. A. Espinosa-Jalapa, D. Milstein, *Angew. Chemie Int. Ed.* **2018**, 12252–12256.

[29] M. Zahmakiran, S. Özkar, *Langmuir* **2009**, *25*, 2667–2678.

[30] M. Zahmakiran, S. Özkar, *Langmuir* **2008**, *24*, 7065–7067.

[31] M. Zahmakiran, Y. Tonbul, S. Özkar, *J. Am. Chem. Soc.* **2010**, *132*, 6541–6549.

[32] S. Smeekens, S. Heylen, N. Janssens, K. Houthoofd, J. A. Martens, C. E. A. Kirschhock, *Chem. Mater.* **2011**, *23*, 4606–4611.

[33] K. K. Bando, H. Arakawa, N. Ichikuni, *Catal. Letters* **1999**, *60*, 125–132.

[34] D. R. Jones, W. A. Al-Masry, C. W. Dunnill, *Sustain. Energy Fuels* **2018**, *2*, 710–723.

[35] F. Ma, M. Wang, L. Jiang, J. Deng, R. Chen, N. Naeve, S. Zhao, *Int. J. Hydrogen Energy* **2010**, *35*, 12502–12509.

[36] C. Zhang, L. Wang, J. Liu, Y. Yang, P. He, Y. Cao, J. Chen, H. Li, *ChemCatChem* **2018**, doi:10.1002/cctc.201800828.

[37] K. Shameli, M. Bin Ahmad, M. Zargar, W. M. Z. W. Yunus, N. A. Ibrahim, *Int. J. Nanomedicine* **2011**, *6*, 331–341.

[38] Y. Zeng, H. Walker, Q. Zhu, *J. Hazard. Mater.* **2017**, *324*, 605–616.

[39] M. Vasić, M. Čebela, I. Pašti, L. Amaral, R. Hercigonja, D. M. F. Santos, B. Šljukić, *Electrochim. Acta* **2018**, *259*, 882–892.

[40] Z. Mojović, P. Banković, N. Jović-Jovičić, A. A. Rabi-Stanković, A. Milutinović-Nikolić, D. Jovanović, *J. Porous Mater.* **2012**, *19*, 695–703.

[41] T. L. Barr, *Appl. Surf. Sci.* **1983**, *15*, 1–35.

[42] P. Frontera, A. Macario, M. Ferraro, P. Antonucci, *Catalysts* **2017**, *7*, 59.

[43] H. Arandiyan, Y. Wang, J. Scott, S. Mesgari, H. Dai, R. Amal, *ACS Appl. Mater. Interfaces* **2018**, *10*, 16352–16357.

[44] B. Z. Zhan, M. A. White, T. K. Sham, J. A. Pincock, R. J. Doucet, K. V. R. Rao, K. N. Robertson, T. S. Cameron, *J. Am. Chem. Soc.* **2003**, *125*, 2195–2199.

Entry for the Table of Contents

TOC TEXT: A nanocrystalline ruthenium catalyst embedded into a zeolite catalyses the hydrogenolysis of cyclic carbonates into glycols and methane. The catalyst displays unprecedented selectivity towards methane, and the reaction may be considered as an extension of the OMEGA process, in which both a valuable liquid and gaseous product are formed.

COMMUNICATION

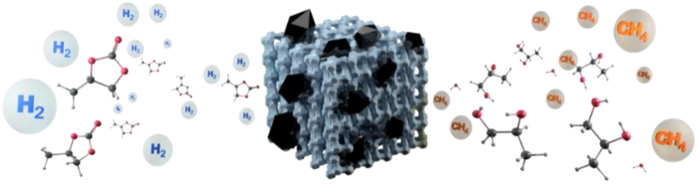

*Wei-Tse Lee, Antoine P. van Muyden, Felix D. Bobbink, Huang Zhangjun, Paul J. Dyson**

Page No. – Page No.

Indirect CO_2 methanation: hydrogenolysis of cyclic carbonates catalyzed by Ru-modified zeolite produces methane and diols